Coupling between motor proteins determines dynamic behaviors of motor protein assemblies

Jonathan W. Driver,[a] Arthur R. Rogers,[a] D. Kenneth Jamison,[a] Rahul K. Das,[b] Anatoly B. Kolomeisky[b] and Michael R. Diehl*[ab]

Received 2nd April 2010, Accepted 27th May 2010
DOI: 10.1039/c0cp00117a

Transport of intracellular cargos by multiple microtubule motor proteins is believed to be a common and significant phenomenon *in vivo*, yet signatures of the microscopic dynamics of multiple motor systems are only now beginning to be resolved. Understanding these mechanisms largely depends on determining how grouping motors affect their association with microtubules and stepping rates, and hence, cargo run lengths and velocities. We examined this problem using a discrete state transition rate model of collective transport. This model accounts for the structural and mechanical properties in binding/unbinding and stepping transitions between distinct microtubule-bound configurations of a multiple motor system. In agreement with previous experiments that examine the dynamics of two coupled kinesin-1 motors, the energetic costs associated with deformations of mechanical linkages within a multiple motor assembly are found to reduce the system's overall microtubule affinity, producing attenuated mean cargo run lengths compared to cases where motors are assumed to function independently. With our present treatment, this attenuation largely stems from reductions in the microtubule binding rate and occurs even when mechanical coupling between motors is weak. Thus, our model suggests that, at least for a variety of kinesin-dependent transport processes, the net 'gains' obtained by grouping motors together may be smaller than previously expected.

Introduction

The transport of organelles and other sub-cellular cargos along polymeric cytoskeletal filaments is critical to mechanisms that regulate the internal organization of eukaryotic cells. These processes are largely driven by molecular motor proteins, active enyzmes that consume ATP as fuel in order to produce the mechanical work necessary to propel sub-cellular commodities within the viscous and highly crowded environments of cells. In recent years, significant attention has been devoted to studying biophysical and biochemical properties of single motor proteins such as kinesins, dyneins and myosins.[1] Yet, there are numerous examples where intracellular transport processes are driven by collections of multiple motor molecules.[2–7] It is often assumed that grouping motors should yield significant gains in motor functionality (*i.e., increased travel lengths, higher force production capabilities, and greater velocities under load*). However, critical issues surrounding multiple motor mechanics have not been resolved, and the precise dependence of most transport parameters on the number of motors responsible for cargo motion remains unclear.

Recent assays and analyses of multiple motor behaviors have become increasingly sophisticated, and have further highlighted the role collective motor mechanics plays in intracellular transport.[1–4,8–10] Nevertheless, transport parameters are often found to depend differently on the number of motors bound to cargos, and in particular, there are significant distinctions between reported *in vivo* and *in vitro* collective behaviors of motor proteins.[5,6,11] Optical trapping experiments have shown that beads coated with multiple kinesins can produce higher forces than those outfitted with single motor molecules.[5] In the same study, cargo run lengths are also found to increase substantially when multiple motors are present. Yet, much less pronounced run length enhancements are observed in other *in vitro* experiments possessing a similar assay format,[11] which leaves questions about the extent to which motors 'benefit' from functioning together. Furthermore, *in vivo* assays of lipid droplet transport that incorporate methods to carefully manipulate and examine the net levels of motors bound to cargo surfaces have shown that neither cargo velocity nor the run length distributions change appreciably with motor copy number.[6] Instead, droplet particles carried by multiple motors were found to move with slightly lower velocities and somewhat smaller run lengths than when single kinesins were responsible for transport. To date, these distinct results have not been reconciled. It may be that the different behaviors observed *in vivo* and *in vitro* stem from unknown regulatory or environmental factors that reduce the enhancements gained by the collective function of motors. However, there are still critical questions regarding the fundamental principles governing the action of multiple motors that must be addressed in order to justify this explanation.

Current understandings of multiple motor function have been advanced by recent theoretical efforts.[12–14] Specifically, a theoretical framework for understanding mechanisms of cooperation between motor proteins has been developed by

[a] *Department of Bioengineering, Rice University, Houston, Texas, USA 77005. E-mail: diehl@rice.edu*
[b] *Department of Chemistry, Rice University, Houston, Texas, USA 77005*

Klumpp and Lipowsky.[12] In their approach, a cellular cargo is driven by a system of motor proteins that can independently bind to or unbind from their microtubule track, and do not interact in any fashion. The system therefore remains associated with the microtubule for longer periods of time, yielding run length enhancements. While this is almost undoubtably qualitatively correct, it seems that the model's quantitative predictions do not explain the diversity of responses reported. Notably, the effects of the structural and mechanical properties of cargos and the linkages that connect motors together are not taken into account, which could influence the lifetime over which a cargo remains attached to a microtubule. Such factors are widely recognized as being important to a host of non-motile, multi-valent biochemical systems, and have been incorporated into more recent computer simulations of multiple motor dynamics.[14] In addition, new data from our laboratory provide more conclusive evidence that interactions between assembly motors alter collective behaviors.[15] Thus, a more comprehensive description of the mechanics and dynamics of multiple motor systems might provide an explanation for experimental observations.

In this paper, we present a new theoretical treatment of multiple motor dynamics that explicitly takes into account mechanical coupling between motors. Using a model experimental system of two coupled kinesin-1 motors as a test case,[15] a solvable discrete state transition rate model of multiple motor dynamics is described that incorporates the relationships between the structural/mechanical properties of multiple motor systems and the rates at which those systems transition between different microtubule-bound configurations (microstates). In agreement with our prior report, we show that the density of microstates where multiple motors drive cargo motion simultaneously can be substantially reduced by interactions between kinesins. These interactions are parameterized as distance-dependent strain energies that arise when two motors must stretch in order to reach their respective microtubule binding sites. The presence of strain energy reduces average cargo run lengths since it results in enhanced motor detachment rates, but also, attenuated motor binding rates. Considering that motors will be coupled together elastically on many biological cargos, our work indicates that fundamental features of multiple kinesin dynamics dictate that cargo transport by multiple kinesins will often be insensitive to kinesin copy number.

Discrete state transition rate model

Model definitions and assumptions

A successful model of multiple motor dynamics must be capable of correctly predicting the relative probabilities of the different configurations in which a system of motors can be bound to its filament track. The microstates available to a system of motors can be generically classified by the number of microtubule-bound molecules (*i.e., 0, 1 or 2 bound motors in a two-kinesin assembly*). As in the previous work,[15] we assume that assemblies will transition between these microstates *via* the binding and unbinding of a single motor within the multi-unit system (Fig. 1). When modeling a system of motors that do not interact, transition rates involving motor detachment can be expressed as $n\varepsilon_1$, where n is the number of bound motors prior to detachment, and ε_1 is the single motor detachment rate. Similarly, motors attach to the microtubule at the single motor binding rate π_0. We consider a transition rate model that relies exclusively on these assumptions to be a '*base-case*' or foundational model that serves as a benchmark to assess the effects of inter-motor communication. To be consistent with the treatments of multi-unit (valent) biochemical systems (*e.g., multivalent ligand–receptor complexes*),[16] we now refer to model predictions derived with these assumptions as collective, but non-cooperative behaviors. The average energy of the bond between a motor and a microtubule in a multi-unit system is identical to that of a single motor, and grouping motors results in neither a net loss, nor a synergistic gain in affinity on a per-motor basis.[17]

The present model is designed to account for basic structural and mechanical properties of assemblies of molecular motors and to allow their relative roles in collective motor function to be assessed. As a test case, we examined the collective dynamics of a structurally-defined motor system composed of two human kinesin-1 motors that we previously developed and studied at the single-assembly level.[15] Motors in this system are organized along a linear molecular scaffold formed from a 50 nm long duplex of DNA. The DNA scaffold in these systems is presently treated as a rigid rod (the persistence length of DNA is 50 nm), while the motors are modeled as linear springs with a specified elastic spring constant (κ_{motor}). The motor linkages can therefore stretch and relax, allowing the assemblies to adopt an array of different microtubule-bound configurations that are differentiated by the spacing between the sites at which each motor is bound to its filament track (Fig. 1). Each configuration of the assembly is enumerated by our model, and is assigned an integer ($i_{2\mathrm{ms}}$) that describes the number of 8 nm distance units that the system is away from an assembly microstate where the net force on each motor is zero (*i.e., the base-case microstate where* $i_{2ms} = 0$*, and the strain energy is zero*). When both assembly motors are microtubule-bound, we assume the motor system can transition between these microstates *via* asynchronous motor stepping, although collective behaviors assuming synchronous stepping were also examined for comparison. Importantly, asynchronous steps change the distance between binding sites of the motors, whereas synchronous steps do not (*i_{2ms} is determined by the binding/unbinding of motors exclusively*). The present treatment also assumes the DNA linkage is always at the same vertical distance from the microtubule, and that all configurations are symmetric with respect to the axis perpendicular to the link and contains its center point (see Fig. 1). This assumption seems reasonable, as kinesins have been shown to maintain their cargo at a specific height above a microtubule during transport ($\sim$17 nm).[18]

Elastic deformations of motor assemblies will cause the free energy of the system to change in time. In the present model, the energies associated with these deformations depend on: (1) the composite elastic compliance of the motor assembly ($\kappa_{\mathrm{assembly}} = 2\kappa_{\mathrm{motor}}$, assuming a net serial spring behavior), and (2) the distance that their linkages are stretched from their equilibrium position (x_i). Each assembly motor can experience

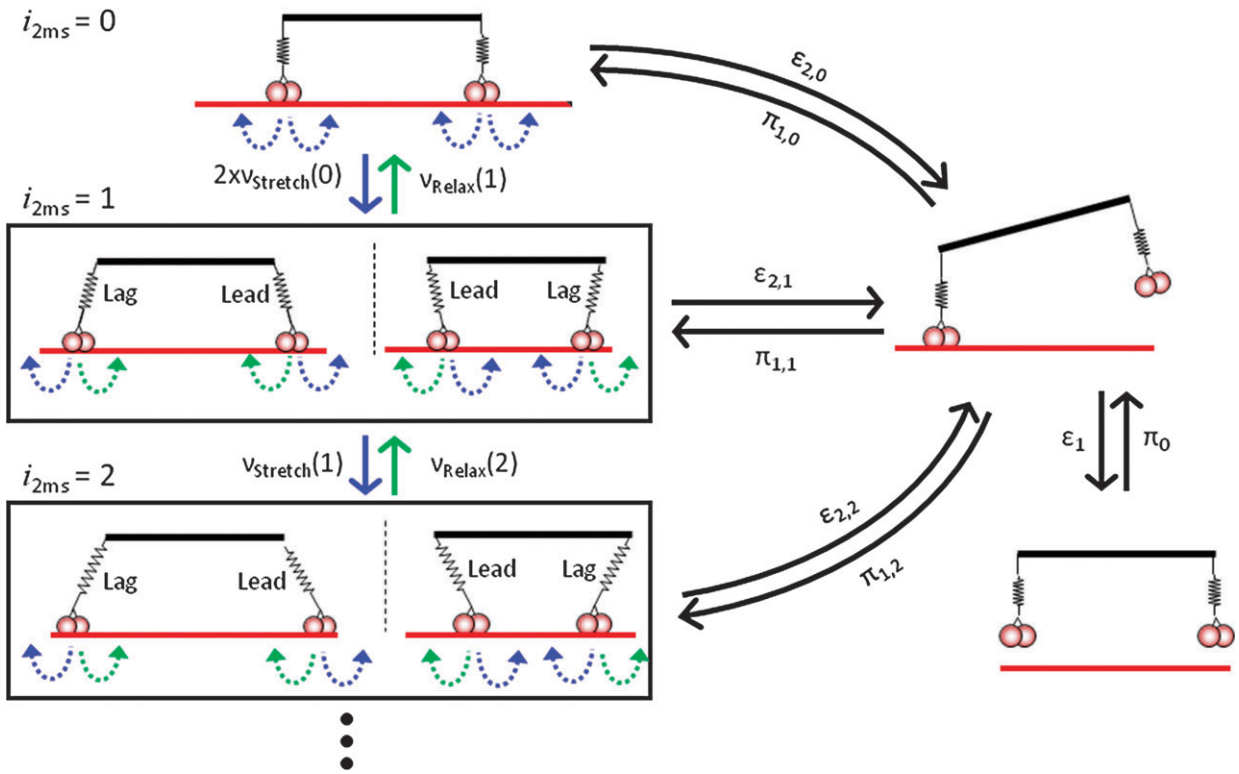

Fig. 1 Schematic representation of the discrete state transition rate model. Degenerate two-motor-bound microstates, enumerated by the index i_{2ms}, are boxed. In each microstate, the leading and lagging motors feel opposing and assisting loads, respectively. A forward step of the leading motor or a backward step of the trailing motor leads to the microstate $i_{2ms} + 1$, while a forward step of the lagging motor or a backward step of the leading motor leads to the microstate $i_{2ms} - 1$. Microstate transitions involving motor stepping are indicated by the solid arrows. The stepping of individual motors is denoted by the dashed arrows. The color coding indicates relationships between the individual motor stepping events and their respective assembly microstate transitions. When $i_{2ms} = 0$, all steps lead to $i_{2ms} = 1$, and $\nu_{stretch} = \nu_{relax}$. The motors unbind out of each i_{2ms} microstate into the single-motor-bound state with a rate $\varepsilon_{2,i}$ and rebind with a rate $\pi_{1,i}$. The single-motor-bound state transitions to the fully unbound state with a rate ε_1, which rebinds with a rate π_0.

either an assisting or opposing force depending on their positions relative to the relaxed, base-case configuration of the assembly (*i.e., they can lead the motion of the assembly or lag behind*). Configurations possessing identical energies are considered to be degenerate; in the absence of an applied load, the "stretched" and "compressed" configurations possessing the same i_{2ms} are treated as identical with respect to strain energy (*these groups of microstates are boxed together in* Fig. 1). In general, states where i_{2ms} is large are considered to be high-strain configurations that introduce energetic costs to the system.

The influence of strain energy on kinetic transitions involving motor–microtubule binding and unbinding was treated by specifying a distinct transition rate into and out of each i_{2ms} microstate configuration according to the following equations:

$$\varepsilon_{2,i} = 2\varepsilon_1 \exp(F(i)/F_d) \quad (1)$$

$$\pi_{1,i} = \pi_0 \exp\left(-\frac{E_2(i) - E_1}{k_b T} + F(i)/F_d\right) \quad (2)$$

In these expressions, π_0 and ε_1 are binding and unbinding rates for a single (*non-interacting*) kinesin motor. The parameter $F(i)$ is the effective horizontal internal force imposed on each motor due to the stretching of the assembly, and F_d is the detachment force,[12] which can be written as $F_d = k_B T/d$. Here, the parameter d can be viewed as the distance between the motor and the microtubule above which the motor is considered to be detached.[19,20] The ratio of forces, $F(i)/F_d$, specifies how strongly the free energy difference between single-bound and double-bound motor states enhances the unbinding transition.[20] Here, motor detachment is assumed to be independent of the vectorial direction of the forces imposed on a motor. The term $E_2(i)$ in eqn (2) is the strain energy of the two-motor system when both motors are bound: $E_2(i) = 1/2\kappa_{assembly}[(8\text{ nm})i_{2ms}]^2$. Note that transition rates involving motor binding are governed by the difference in the energies of the assembly when they adopt a microstate where one motor is unbound and its linkages are relaxed ($E_1 = 0$), and those where the assembly must stretch to reach between two specific microtubule sites; we consider the motor bound when the assembly is stretched a distance ($8i_{2ms} - d$). Importantly, these transitions are driven exclusively by thermal energy, and therefore, transition rates into microstate configurations possessing high strain energies will be lower than transition rates into microstates where the motor linkages are not stretched far from their relaxed positions. Furthermore, while allowing a more microscopic description of the dynamics of motor protein assemblies to be developed, our treatment of energetic costs associated with the binding and unbinding of assembly motors and transitions between microstates satisfies detailed balance.

Individual motor stepping rates are determined using an analytical solution to a two-state kinetic model of kinesin dynamics.[19,20] This model was chosen over other empirical treatments since it not only captures kinesin's non-linear $F - V$ dependence, but it should also provide a framework for future assessments of perturbations to a motor's mechano-chemical properties that may arise due to specific forms of inter-motor coupling. Herein, we use this model to specify microstate-dependent forward and reverse stepping rates for the motors ($\nu_{i,+}$ and $\nu_{i,-}$). Although the ATP-stimulated motion of motor proteins along the microtubule is a complex multi-step process, for simplicity, we model motor stepping with only two effective rates, $\nu_{0,+}$ and $\nu_{0,-}$. The velocity of an assembly when only one motor is microtubule-bound is calculated using: $V_1 = (8\text{ nm})(\nu_{0,+} - \nu_{0,-})$. Strain energy due to inter-motor coupling when both motors are bound is assumed to influence motor stepping according to:

$$\nu_{i,+} = \nu_{0,+} e^{\frac{-\theta(E_{2(i+1)} - E_{2(i)})}{k_B T}} \quad (3)$$

$$\nu_{i+1,-} = \nu_{0,-} e^{\frac{(1-\theta)(E_{2(i+1)} - E_{2(i)})}{k_B T}} \quad (4)$$

where the coefficient θ describes the splitting of the effect of free energy difference on transition rates between microstates. To simplify calculations, we assumed that $\theta = 0.10$. Such treatment captures both kinesin's non-linear $F - V$ dependence and low probability for backward stepping when the forces imposed on a motor due to inter-motor strain are small ($F_{\text{strain}} < F_{\text{stall}}$).[21]

The instantaneous velocity of each motor in the system is determined by the difference between their forward and backward stepping rates, defined in eqn (3) and (4). However, in order to construct the master equations, we need expressions for the rates of transition between microstates, which are defined by their energy. In each microstate, either a forward step of the leading motor or a backward step of the lagging motor leads to the $i_{2\text{ms}} + 1$ microstate. Conversely, a backward step of the leading motor or a forward step of the lagging motor will lead to the $i_{2\text{ms}} - 1$ microstate. We therefore define the transition rates between different microstates as: $\nu_{\text{stretch}}(i) = [(\nu_{i,+})_{\text{lead}} + (\nu_{i,-})_{\text{lag}}]$ and $\nu_{\text{relax}}(i) = [(\nu_{i,-})_{\text{lead}} + (\nu_{i,+})_{\text{lag}}]$.

Estimations of the collective transport parameters

Before calculating collective transport parameters of interest, the assumptions described above are first used to determine the relative densities of each relevant microstate configuration of the two-motor system by solving the following master equations:

$$\partial_t \psi_0 = \varepsilon_1 \psi_1 - \pi_0 \psi_0 \quad (5)$$

$$\partial_t \psi_1 = \pi_0 \psi_0 + \Sigma_{i=0}^{N} \varepsilon_{2,i} \psi_{2,i} - (\varepsilon_1 + \Sigma_{i=0}^{N} \pi_{1,i}) \psi_1 \quad (6)$$

$$\partial_t \psi_{2,i} = \pi_{1,i} \psi_1 + \nu_{\text{stretch}}(i-1)\psi_{2,i-1} + \nu_{\text{relax}}(i+1)\psi_{2,i+1} - [\varepsilon_{2,i} + \nu_{\text{stretch}}(i) + \nu_{\text{relax}}(i)]\psi_{2,i}. \quad (7)$$

Here, ψ_n denotes the probability that an assembly adopts a configuration possessing n filament-bound motors. When $n = 2$, ψ_n gains an additional index (i) which specifies the binding-site distance between the two assembly motors as described above. In eqn (7), the densities of individual assembly configurations are modulated *via* motor binding, detachment and stepping.

With predicted microstate densities, the 'effective' rates describing how rapidly an assembly transitions between the general classes of assembly microstates can be calculated *via*:

$$\pi_{1,\text{eff}} = \Sigma \pi_{1,i} \quad (8)$$

$$\varepsilon_{2,\text{eff}} = \frac{\sum \varepsilon_{2,i} \psi_{2,i}}{\sum \psi_{2,i}} \quad (9)$$

Here, the 'effective' rate of assembly transitions from single into all possible two motor-bound configurations ($i_{2\text{ms}}$ microstates) is simply the sum of all individual enumerated binding rates. The 'effective' dissociation rate of a motor from microstates where both motors are bound ($\varepsilon_{2,\text{eff}}$) is taken as the population-weighted average of the dissociation rates out of these microstates, and accounts for the relative probabilities of each unique configuration explicitly. These weightings also influence the average force imposed on each motor ($F_{2,\text{av}}$), the average system velocity (V_{av}), and the total effective dissociation rate of a two-motor system ($\varepsilon_{\text{system}}$)[12] as specified by:

$$F_{2,\text{av}} = \frac{\sum F_{2,i} \psi_{2,i}}{\sum \psi_{2,i}} \quad (10)$$

$$V_{\text{av}} = \frac{\sum V_{2,i} \psi_{2,i} + V_1 \psi_1}{\sum \psi_{2,i} + \psi_1} \quad (11)$$

$$\varepsilon_{\text{system}} = \frac{\varepsilon_2}{(1 + [\pi_{1,\text{eff}}/\varepsilon_{2,\text{eff}}])}. \quad (12)$$

In eqn (11), the microstate velocity $V_{2,i}$ is calculated using: $V_{2,i} = (4\text{ nm})\{[(\nu_{i,+})_{\text{lead}} - (\nu_{i,-})_{\text{lead}}] + [(\nu_{i,+})_{\text{lag}} - (\nu_{i,-})_{\text{lag}}]\}$. Here, we assume that the motors step asynchronously and use a fractional motor displacement size to account for the stretching of the assembly linkages. Potential enhancements or net-losses in collective motor function relative to the non-cooperative model behaviors can be evaluated by examining the ratios $\pi_{1,\text{eff}}/\pi_{1,0}$, $\varepsilon_{2,\text{eff}}/\varepsilon_{2,0}$, and V_{av}/V_0, where $\pi_{1,0}$, $\varepsilon_{2,0}$, and V_0 correspond to the binding/unbinding rates and cargo velocities expected when motors function non-cooperatively. Similarly, whether the structural/mechanical properties of multiple motor systems lead to deviations from idealized (*non-interacting*) behaviors can be assessed by examining RL/RL_0, where average predicted run lengths in each case are calculated *via* $\text{RL} = V/\varepsilon_{\text{system}}$.

Finally, the relative influence of motor stepping and binding/unbinding kinetics on multiple motor dynamics was examined by comparing two-motor microstate distributions and transition rates produced when the motors are assumed to advance either synchronously or asynchronously; synchronous stepping was treated by eliminating stepping transitions between microstates from eqn (7). In each case, the master equations for the two motor systems are defined using measured single-kinesin and collective transport parameters obtained from our previous analyses of two-kinesin run length distributions (Table 1).[15]

Table 1 Measured and assumed model parameters

Measured constants (single motor)		Measured/predicted constants (two motor)			Mean field[a]	Discrete microstate model[b]
ε_1	0.61 s^{-1} [a]	$\kappa_{assembly}$	0.025 pN nm^{-1}	$\varepsilon_{2,eff}$	$\sim$4 s^{-1}	1.47 s^{-1}
π_0	4.7 s^{-1} [c]	$RL_{0(predicted)}$	3.9 μm[c]	$\pi_{1,eff}$	$\sim$2.5 s^{-1}	0.67 s^{-1}
κ_{mot}	0.05 pN nm^{-1} [d]	$RL_{(measured)}$	1.4 μm[a]	$\pi_{1,eff}/\varepsilon_{2,eff}$	0.625	0.46
$RL_{(measured)}$	0.83 μm[a]			F_c or $F_{2,av}$	3.6 pN	0.52 pN
				$RL_{(predicted)}$	—	1.17 μm

[a] Results from fits reported in ref. 15. [b] Values are calculated assuming motors advance *via* asynchronous stepping. [c] Non-cooperative run lengths RL_0 were determined using eqn (10), assuming measured two-motor velocities and single-motor detachment rate for ε_1.[12] The 'partial' two-motor detachment rate was calculated assuming $\varepsilon_2 = 2\varepsilon_1$. The intrinsic binding rate π_0 is adopted from previous reports.[3,12] [d] Determined from optical trapping experiments performed in-house. The elasticity of our polymer linked kinesins actually increases non-linearly with force due to strain-induced stiffening (*e.g.*, κ_{mot} increases from 0.05 pN nm^{-1} to approximately 0.2 pN nm^{-1} sharply around an applied load of 2.5 pN).

Results and discussion

Predicted stationary-state distributions of i_{2ms} microstates for a two-kinesin assembly calculated over a large range of assembly (motor) elasticities are shown in Fig. 2. Two general collective behaviors are revealed by these analyses, both of which appear to be largely independent of the mechanism by which the motors are assumed to advance forward. First, it is shown that assembly microstates where two motors are filament-bound are much less prevalent than the single-motor-bound configuration ($\psi_1 > \Sigma\psi_{2,i}$). Furthermore, the total probability that a motor assembly will adopt two-motor-bound microstates ($\psi_2 = \Sigma\psi_{2,i}$) is substantially lower than model predictions where motors behave non-cooperatively, even when the assembly elasticity is small (Fig. 2, inset). Secondly, as expected, when the assembly is mechanically compliant (*i.e.*, *when* κ_{motor} *is small*), higher probability densities $\psi_{2,i}$ are found for assembly configurations where the i_{2ms} separation distance is large. Yet, for all values of κ_{motor} examined, there is a general tendency for the two motor systems to occupy microstate configurations close to the $i_{2ms} = 0$ microstate of the system; note the 'offset' peak as $i_{2ms} = 1$ stems from the fact that there are two degenerate configurations where the motors can be separated by 8 nm from the relaxed state, and that there is only one where the motors do not experience forces due to strain ($i_{2ms} = 0$).

The low probability of assembly configurations where both motors are filament-bound is reflected in the effective binding and unbinding transition rates $\pi_{1,eff}$ and $\varepsilon_{2,eff}$ (Fig. 3); $\pi_{1,eff}$ decreases rapidly with increasing κ_{motor}. Such behavior is expected, as a stiffening of motor–motor linkages should reduce the number of sites to which a motor can bind when its partner is already filament-bound. Thus, the effective concentration of lattice sites available to an unbound assembly motor will be lower in circumstances where they are incorporated into multi-unit assemblies that are rigid compared to those that are more mechanically compliant. While this behavior should not depend on how motors advance once they are filament bound, motor stepping mechanisms are found to play a role in determining the effective detachment rate $\varepsilon_{2,eff}$. When the motors step asynchronously, $\varepsilon_{2,eff}$ is found to increase with increasing κ, and is consistently larger than the values predicted from assumptions of non-cooperative behavior ($\varepsilon_2 = 2\varepsilon_1$). Importantly, this behavior is accompanied by an increase in the average effective force ($F_{2,av}$) experienced by each microtubule-bound motor in the system. However, $F_{2,av}$ does not increase indefinitely with increasing κ since i_{2ms} microstates possessing high strain energy become increasingly improbable.

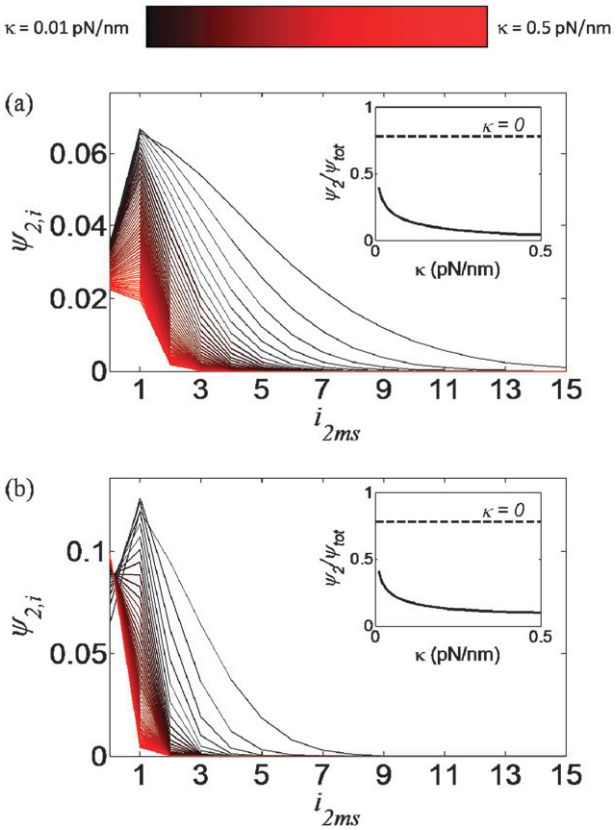

Fig. 2 Population distributions of two-motor-bound microstates i_{2ms} for (a) asynchronous stepping and (b) synchronous stepping for various values of the assembly stiffness. The sum of the two-motor-bound microstate populations *versus* stiffness is shown in the inset.

Despite the fact that motors can impose relatively high forces (pN-sized) on one another, the development of these forces appears to have little impact on average two-motor velocities. This result is also explained by the low densities of microstates where two motors are bound, which occurs due to the low binding rates and high detachment rates of the motors within the system, especially for configurations where the i_{2ms} distance is large. Nevertheless, microstate distributions are not

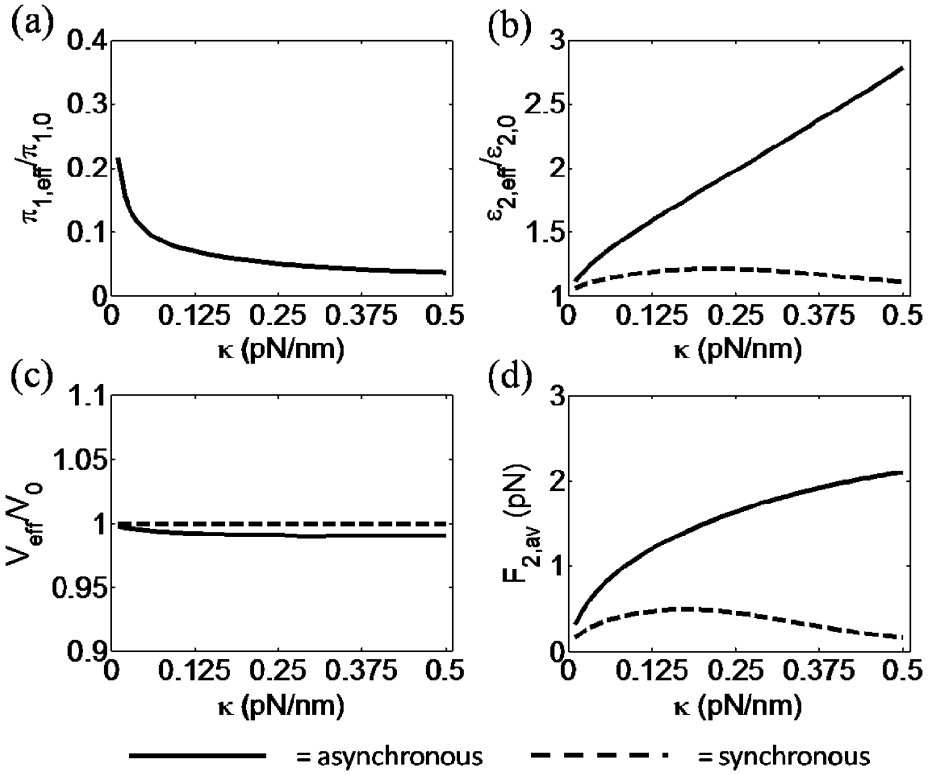

Fig. 3 Transport parameters of interest as a function of assembly stiffness: (a) normalized effective binding rate, (b) normalized effective dissociation rate, (c) normalized average velocity, and (d) average internal force in the two-motor-bound microstates. The solid line in each plot represents the values derived from the model including asynchronous stepping, while the dashed line represents the synchronous case. The dashed line denoting synchronous stepping is not visible in the binding rate plot since it is superimposed on the solid, asynchronous line.

governed by motor attachment/detachment kinetics alone. Asynchronous motor stepping behavior is found to increase the probability that the system will adopt configurations with large i_{2ms} separation distances compared to those predicted for a set of synchronized motors. Here, since the motors do not advance at the same time, there is a finite probability that the motor separation distance that is produced upon motor binding will increase due to the advancement of a leading motor. Thus, stochastic fluctuations in motor stepping can lead to a broadening of the binding site separation distances, and in turn, much higher strain energies. While such behavior appears to be general, the influence of motor stepping on microstate distributions was found to depend on the chosen value of θ assumed in our model for kinesin $F - V$ dependence (eqn (3) and (4)), and was most influential when θ is assumed to be small (*i.e. when low-force, backward stepping rates are nearly negligible*).

Perhaps most importantly, while the average run lengths are generally expected to increase with increasing motor number, our model suggests that run length enhancements stemming from grouping motors can be attenuated significantly when strain energy influences motor–microtubule binding and detachment. This suggestion is bolstered by the fact that the model predicts the average run length of our experimental system much more accurately than a non-interacting model (Table 1). Furthermore, reductions in run lengths compared to non-cooperative behaviors, as indicated by the calculated ratio RL/RL_0 (Fig. 4), are found to occur despite the assumed mechanism of motor stepping. Such behavior is consistent with the present predictions that the single-motor-bound configuration of the two-motor assembly constitutes the dominant microstate of the system. Thus, unless cargo–motor linkages are exceptionally compliant, the run length enhancements predicted by 'base-case', non-cooperative models of multiple motor mechanics will likely not be realized ($RL/RL_0 = 0.5$ when $\kappa_{motor} \approx 0.005$ pN nm^{-1}). Our experimental system in Rogers *et al.* consisted of recombinant kinesin motors coupled to a DNA duplex *via* highly compliant protein-based polymers,[15] and thus, this system is likely as or perhaps even more compliant than many multiple motor complexes found *in vivo*. Furthermore, cargos that are even more flexible should exhibit appreciable strain-induced stiffening, and therefore, once motors are separated by relatively large i_{2ms} distances, strain energy of multiple motor bound microstates will likely impact multiple motor behaviors.

The general agreement between calculated average run lengths when motors advance *via* either asynchronous or synchronous stepping suggests that transitions involving motor binding can impact collective behaviors more significantly than motor detachment. This behavior is explained by the tendency for the two-motor system to move with only a single filament-bound motor; the rate for assembly transition out of the 'single-motor' configuration is slow. Accordingly, increases in the 'effective' transition rate $\varepsilon_{2,eff}$ are much less influential since such effects occur in the minority microstates of the system. Thus, even though the average internal force $F_{2,av}$ is much

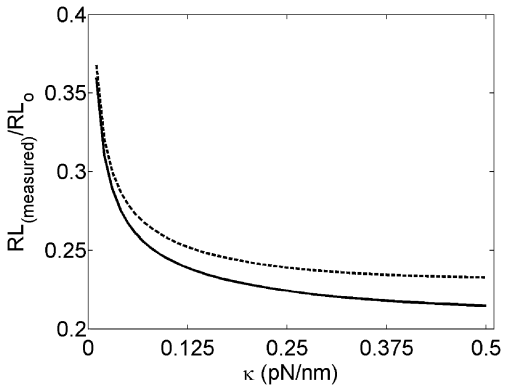

Fig. 4 Normalized average run length *versus* system stiffness (κ) for asynchronous (solid) and synchronous (dashed) motors. The non-cooperative, base case behavior corresponds to $\kappa = 0$, where $RL_{measured}/RL_0 = 1$.

higher in the two-motor system when motors are assumed to step asynchronously, the presence of these forces only results in a slight drop in the average run length and velocity of the system over predictions where the motors advance *via* synchronous stepping.

Consistent with the model's predictions, we have previously shown that grouping two kinesin-1 motors together does not lead to the run length enhancements expected from non-cooperative model predictions (Table 1). Analyses of these experimental results have shown that models assuming non-cooperative behaviors ($\varepsilon_2 = 2\varepsilon_1$) yield inadequate fits to two-motor run length data unless the value for the single-motor binding rate (π_0) is used as an adjustable parameter; agreement is only achieved if the binding rate is much lower than the values that are typically assumed in most reports: $\pi_0 \approx 1\ s^{-1}$ instead of $\pi_0 = 4.7\ s^{-1}$. Although the lowering of the binding rate appears to be consistent with our present picture of multiple kinesin dynamics, we consider this treatment to be physically unrealistic since some form of inter-motor interactions would likely be necessary to explain such an effect (*i.e. motors should be able to bind rapidly unless there are explicit reasons for the attenuation of their attachment rates; we note that earlier estimates of π_0 came from experiments where motors could freely diffuse on their cargo (lipid tubules)*[3] *and although there may be subtle differences in the system geometry that still need to be considered, π_0 is likely approximated reasonably*). In our prior report, we attempted to reconcile this issue by assuming that the assembly motors experience a mean-field force due to the stretching of motor linkages when both motors are filament-bound. Here, the forces due to strain, or 'counter-forces' (F_c), were incorporated into the effective detachment rate $\varepsilon_{2,eff}$, and should be considered as a mean-field force developed within the motor system since configuration-dependent forces are not modeled explicitly. It seemed counterintuitive to assume strain energy affects motor binding, and such effects were not included in our analyses. With this treatment, run length data can be fit while using intrinsic single-motor binding rates that appear to be more reasonable ($\pi_0 \approx 2.5\ s^{-1}$). However, such agreement required counter forces that were larger than those generally expected for the experimental system ($F_c = 3.6$ pN).

By incorporating strain energy in the motor binding and detachment, our present analyses allow further refinement of this result. Here, the assumption of high intrinsic single-motor attachment rates ($\pi_0 \approx 4.7\ s^{-1}$) can still be employed, but if motor–filament binding is attenuated by intrinsic structural and mechanical properties of the assemblies, the reduction in the effective binding rate $\pi_{1,eff}$ lessens the role of motor detachment in collective behaviors. As a result, agreement with experimental measurements of the assembly's average run length is found with significantly lower values for $F_{2,av}$ (*e.g., an assumed effective spring $\kappa_{motor} = 0.05\ pN\ nm^{-1}$ yields the measured average two-motor run length and a 'counter-force' that is ~0.5 pN*).

Conclusions

We have developed a discrete state transition rate model of multiple motor dynamics that allows more detailed assessments of how a motor assembly's structural and mechanical properties influence its collective transport. In the present form of this model, such properties are incorporated by specifying strain-dependent motor–microtubule attachment and detachment rates. Compared to treatments where non-cooperative behaviors are assumed, or where a mean-field force is considered to only affect motor detachment, the explicit treatment of strain-energy in expressions describing the rates at which motors within assemblies bind into and detach from specific microtubule-bound configurations provides more physically realistic predictions of effective rates that assemblies will transition between general classes of microstates (*possessing different numbers of filament-bound motors*). Overall, these analyses show that the enhancements obtained by grouping multiple motors are much less significant than those expected from 'base-case', non-cooperative models. Such behavior is consistent with run length measurements of structurally-defined systems of multiple kinesin-1 molecules, and may also provide an explanation for why kinesin copy number does not seem to influence *in vivo* cargo run lengths appreciably. In both cases, we predict that small systems of kinesins will most commonly transport their cargo primarily *via* a single microtubule-bound motor.

Although a group of motors working against small loads is generally expected to advance *via* asynchronous stepping, our comparison of different stepping mechanisms revealed the importance of characterizing inter-relationships between mechanical properties of motor assemblies and effective motor–microtubule binding rates. Such behavior may have implications for cargo transport in cells. For example, the non-motile microtubule associated protein tau has been shown to reduce the rate that kinesin motors bind to microtubules, but does not to influence kinesin's stepping or detachment rates. Consequently, tau is believed to reduce the run lengths of cargos that are transported by multiple kinesins, but not single kinesin molecules.[22] Yet, if a multiple motor system already possesses an intrinsic tendency to transport its cargo while only using a small fraction of the total number of its surface-bound motors, tau's effect on cargo motion would be diminished. Thus, the organization of motors on cargos and their intrinsic mechanical properties may not only influence

mechanisms of multiple motor transport, but also potential responses to non-motile factors that regulate cargo motility. While validating such ideas ultimately requires further development of experimental methods and refinement of existing theoretical models, recent advances from our group and others are now making such detailed analyses increasingly possible.

Acknowledgements

This work was supported by NSF IGERT fellowships (to DKJ and JWD), an NIH fellowship (to DKJ) and grants from the NSF (MCB-0643832 to MRD; ECCS-0708765 to ABK) and the Welch Foundation (C-1625 to MRD; C-1559 to ABK).

References

1 R. Vale, *Cell*, 2003, **112**, 467.
2 M. Vershinin, B. C. Carter, D. S. Razafsky, S. J. King and S. P. Gross, *Proc. Natl. Acad. Sci. U. S. A.*, 2007, **104**, 87.
3 C. Leduc, O. Campas, K. B. Zeldovich, A. Roux, P. Jolimaitre, L. Bouret-Bonnet, B. Goud, J.-F. Joanny, P. Bassereau and J. Prost, *Proc. Natl. Acad. Sci. U. S. A.*, 2004, **101**, 17096.
4 V. Levi, A. S. Serpinskaya, E. Gratton and V. Gelfand, *Biophys. J.*, 2006, **90**, 318.
5 A. Kunwar, M. Vershinin, J. Xu and S. P. Gross, *Curr. Biol.*, 2008, **18**, 1173.
6 G. T. Shubeita, S. L. Tran, J. Xu, M. Vershinin, S. Cermelli, S. L. Cotton, M. A. Welte and S. P. Gross, *Cell*, 2008, **135**, 1098.
7 V. Soppina, A. K. Rai, A. J. Ramaia, P. Barak and R. Mallik, *Proc. Natl. Acad. Sci. U. S. A.*, 2009, **106**, 19381.
8 J. L. Ross, H. Shuman, E. L. Holzbaur and Y. E. Goldman, *Biophys. J.*, 2008, **94**, 3115.
9 C. Leduc, F. Ruhnow, J. Howard and S. Diez, *Proc. Natl. Acad. Sci. U. S. A.*, 2007, **104**, 10847.
10 J. A. Laib, J. A. Marin, R. A. Bloodgood and W. H. Guilford, *Proc. Natl. Acad. Sci. U. S. A.*, 2009, **106**, 3190.
11 J. Beeg, S. Klumpp, R. Dimova, R. S. Gracia, E. Unger and R. Lipowsky, *Biophys. J.*, 2008, **94**, 532.
12 S. Klumpp and R. Lipowsky, *Proc. Natl. Acad. Sci. U. S. A.*, 2005, **102**, 17284.
13 M. J. I. Muller, S. Klumpp and R. Lipowsky, *Proc. Natl. Acad. Sci. U. S. A.*, 2008, **105**, 4609.
14 A. Kunwar and A. Mogilner, *Phys. Biol.*, 2010, **7**, 016012.
15 A. R. Rogers, J. W. Driver, P. E. Constantinou, D. K. Jamison and M. R. Diehl, *Phys. Chem. Chem. Phys.*, 2009, **11**, 4882.
16 M. Mammen, S.-K. Choi and G. M. Whitesides, *Angew. Chem., Int. Ed.*, 1998, **37**, 2754.
17 P. E. Constantinou and M. R. Diehl, *J. Biomech.*, 2010, **43**, 31.
18 J. Kerssemakers, J. Howard, H. Hess and S. Diez, *Proc. Natl. Acad. Sci. U. S. A.*, 2006, **103**, 15812.
19 M. E. Fisher and A. B. Kolomeisky, *Proc. Natl. Acad. Sci. U. S. A.*, 2001, **98**, 7748.
20 A. B. Kolomeisky and M. E. Fisher, *Annu. Rev. Phys. Chem.*, 2007, **58**, 675.
21 T. Schmeidl and U. Seifert, *Europhys. Lett.*, 2008, **83**, 30005.
22 R. Dixit, J. L. Ross, Y. E. Goldman and E. L. F. Holzbaur, *Science*, 2008, **319**, 1086.